

CN 026

COLUMN LEACHING OF TRACE METALS FROM
DULUTH GABBRO MATERIAL

by

Neil Carriker
Steven Eisenreich
Department of Civil and Mineral Engineering
University of Minnesota
Minneapolis, MN 55455

Report Submitted To:

Minnesota State Planning Agency
Minnesota Environmental Quality Board
Cu-Ni Regional study

July 1978

LIST OF FIGURES

- Figure 1: Nickel vs time (all six)
- Figure 2: Cobalt vs time (all six)
- Figure 3: MN vs time (all six)
- Figure 4: Sulfate vs time (all six)
- Figure 5: Ni vs time (Unmineralized only)
- Figure 6: Co vs time (Unmineralized only)
- Figure 7: Cu vs time (all six)
- Figure 8: Fe vs time (all six)

Introduction

Batch leaching experiments have been a major focus of the investigations of heavy metal leaching from minerals found in northeastern Minnesota. Such experiments provide much useful information about maximum leaching rates and mechanisms by which metals are released from minerals. However, the conditions used in batch leaching studies usually do not even approach typical conditions encountered in real-world situations. Furthermore, these studies are short-term compared to the amount of time a mineral stockpile might be exposed to the elements. While well-designed batch studies may provide essential information, one must be cautious about extrapolating the results to real situations. A need exists for another type of investigation more closely paralleling the actual situation to supplement the batch leaching results and to provide a basis for predicting leaching behavior of mineral stockpiles.

The column leaching experiments described here were designed to provide some of this additional information. The principal objectives of these studies were to:

1. Evaluate the long-term leaching rates of mineralized and unmineralized Duluth Gabbro material.
2. Evaluate the effects of different types of leaching solutions on leaching rates and concentrations of metals in leachates.
3. Evaluate the possibility that prolonged leaching might produce enough acid through oxidation and hydrolysis of exposed iron sulfide minerals to exceed the buffering capacity of the aluminum silicate matrix and result in acidic leachates.

Experimental Design

Three pairs of 5 cm x 100 cm glass columns were set up in a constant temperature room (20°C). One column in each pair was packed with 3 kg of 3/8 mesh (1/4"-1/10" diameter pebbles) mineralized gabbro and the other column was packed with 3/8 mesh unmineralized gabbro. Both gabbro samples were obtained from Erie Mining Company's Dunka Pit. This filled each column to within 10-20 cm of the top. One pair of columns was leached with distilled water to simulate rainwater, a second pair was leached with a synthetic groundwater characteristic of the groundwater in northeastern Minnesota, and the third pair was leached with a synthetic surface water. Leachate application rates of 0.1 ml/min were regulated by the pressure drops through 25 cm sections of 26 gauge stainless steel needle stock. Leachates were collected continuously in 1 l polyethylene bottles and samples were taken at various intervals for sulfate, pH, and metals analyses. Compositions and preparations of the synthetic groundwater and surface water solutions were as follows:

Surface Water:

11.2 mg/l Na ⁺	26. mg CaCO ₃	
2.0 mg/l K ⁺	1.1 ml 0.1 M H ₂ SO ₄	1) Dissolve CaCO ₃
8.2 mg/l Ca ⁺⁺	2.2 ml 0.1 M HCl	in acid
5.0 mg/l Mg ⁺⁺		
25.0 mg/l HCO ₃ ⁻	40.5 mg Na ₂ SiO ₃ .9 H ₂ O	2) Dissolve in H ₂ O,
8.0 mg/l Cl ⁻	3.8 mg KCl	dilute to 750 ml
11.3 mg/l SO ₄ ⁼	1.2 mg K ₂ HPO ₄ .3 H ₂ O	add to (1)
4.0 mg/l SiO ₃ ⁼ (as Si)		
10.0 mg/l Tannic Acid (as C)	18 mg Tannic Acid	3) Dissolve acid
5.0 mg/l Citric Acid (as C)	20 mg Sodium Citrate.2 H ₂ O	add
26.0 mg/l NO ⁻		
0.5 mg/l PO ₄ ⁼	53.4 mg Mg(NO ₃) ₂	4) Dissolve, add, adjust to pH 7, dilute to 1 liter

Groundwater:

24.5 mg/l Na^+	37.5 mg CaCO_3	1)	
2.0 mg/l K^+	4.0 ml 0.1 M H_2SO_4		
15.0 mg/l Ca^{++}			
25.0 mg/l Mg^{++}	50.7 mg $\text{Na}_2\text{SiO}_3 \cdot 9\text{H}_2\text{O}$		Same sequence
46.0 mg/l HCO_3^-	3.8 mg KCl	2)	as for surface
36.0 mg/l $\text{SO}_4^{=}$	1.2 mg $\text{K}_2\text{HPO}_4 \cdot 3\text{H}_2\text{O}$		water.
1.8 mg/l Cl^-			
5.0 mg/l $\text{SiO}_3^{=}$ (as Si)	267 mg $\text{Mg}(\text{NO}_3)_2 \cdot 6\text{H}_2\text{O}$	3)	
129 mg/l NO_3^-			
0.5 mg/l $\text{PO}_4^{=}$			

Results and Discussion

Shortly after initiation of the leaching experiments it became apparent that control of the synthetic groundwater and surface water flow rates would be difficult. Both solutions, especially the surface water, proved to be excellent growth media for bacteria. It was nearly impossible to keep the solutions free of bacteria which sloughed off the transfer lines and clogged the 26 gauge needle stock flow regulators. Addition of 0.5% (V/V) chloroform to the formula, along with filtration through 0.45 μm membrane filters helped control bacterial growth, but did not eliminate the problem entirely. In addition, the original groundwater recipe had 15 mg/l Si which led to formation of crystalline precipitates which clogged the flow regulators.

Analysis of the collected leachates showed that as in the batch studies, the buffer capacity of the mineral matrix was sufficient to maintain neutral pH values in the leachates throughout the investigation. This observation suggests that it is only a remote possibility that long-term leaching of gabbro stockpiles will produce acid leachates in northeastern Minnesota.

Concentrations of sulfate and heavy metals were much higher in the column leachates than in the batch leachates. The values were much more comparable to those observed in samples collected in the field. A probable cause for the higher concentrations is that the effective ratios of weight gabbro/volume leachate and surface area gabbro/volume leachate were much greater in the column studies than in the batch studies; for comparable weights of gabbro, much smaller volumes of leachate came into contact with the mineral in the column studies.

When the results are plotted as cumulative weights of each parameter leached as a function of time, two principal groups emerge. Nickel, cobalt, manganese, and sulfate exhibit greater variations in leaching behavior between types of gabbro (mineralized vs unmineralized) than between types of leaching solutions (groundwater vs surface water vs rainwater). Conversely, copper and iron exhibit greater variations between leachants than between types of gabbro.

The pronounced difference between types of gabbro in the first group of parameters is apparent in Figures 1-4. The column containing mineralized gabbro and leached with groundwater consistently exhibited the highest leaching rates. The two systems containing mineralized gabbro and leached with surface water and rainwater had comparable leaching rates for each of these parameters. These rates were somewhat smaller than those observed for the groundwater/mineralized system, but were significantly greater than for the three unmineralized gabbro systems. The lower three curves in these figures correspond to the unmineralized gabbro systems; it is apparent that the primary difference in leaching behavior observed for Ni, Co, Mn and $\text{SO}_4^{=}$ is attributable to differences between types of gabbro rather than to differences in leaching solutions. However, examining these figures along with the expanded-scale presentation

of the unmineralized results for Ni and Co (Figures 5 and 6), the following order of effectiveness of leachants is observed with both types of gabbro:

groundwater > surface water > rainwater

The one exception to this trend occurs with sulfate, where the order of surface water and rainwater are reversed.

Natural groupings of the curves presenting the results for Cu and Fe is less obvious than for the other four parameters. Close examination of Figures 7 and 8 reveals that the type of leaching solution is the principal factor affecting leaching behavior of these two elements. The synthetic surface water was most effective in leaching both Cu and Fe from both types of gabbro (upper two curves in each figure), followed by the groundwater (middle two curves), with the rainwater being least effective. Differences between the mineralized and unmineralized gabbro were relatively small, although in most cases the mineralized gabbro had the higher leaching rate in each pair.

The table below presents the overall leaching rates on an annual basis observed in these column leaching studies. The values observed here are comparable to those observed in field investigations, reaffirming the validity of this approach to leaching investigations.

Overall Annual Leaching Rates ($\mu\text{g}/\text{kg}$ gabbro/yr) Observed in This Study

	<u>Mineralized Gabbro</u>			<u>Unmineralized Gabbro</u>		
	<u>Groundwater</u>	<u>Surface Water</u>	<u>Rainwater</u>	<u>Groundwater</u>	<u>Surface Water</u>	<u>Rainwater</u>
Ni	17,400	10,060	7,740	508	197	13.3
Co	832	432	389	26.4	9.76	2.45
Mn	1,830	1,202	776	268	146	20.2
SO ₄ ⁼	539,000	217,000	207,000	398,000	169,000	107,000
Cu	36.3	87.8	13.2	28.9	145	7.54
Fe	111	380	17.3	139	235	104

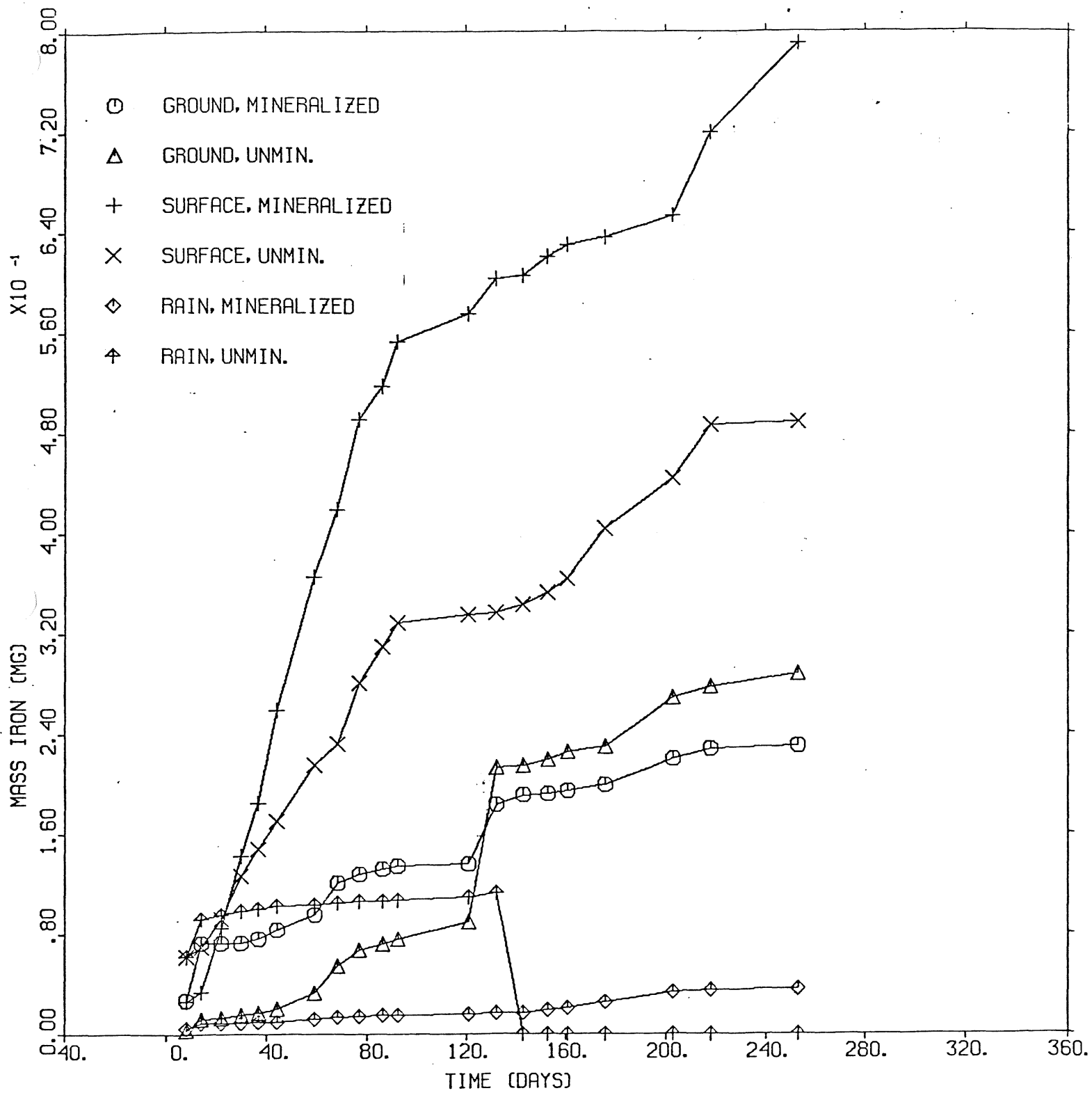
Summary and Conclusions

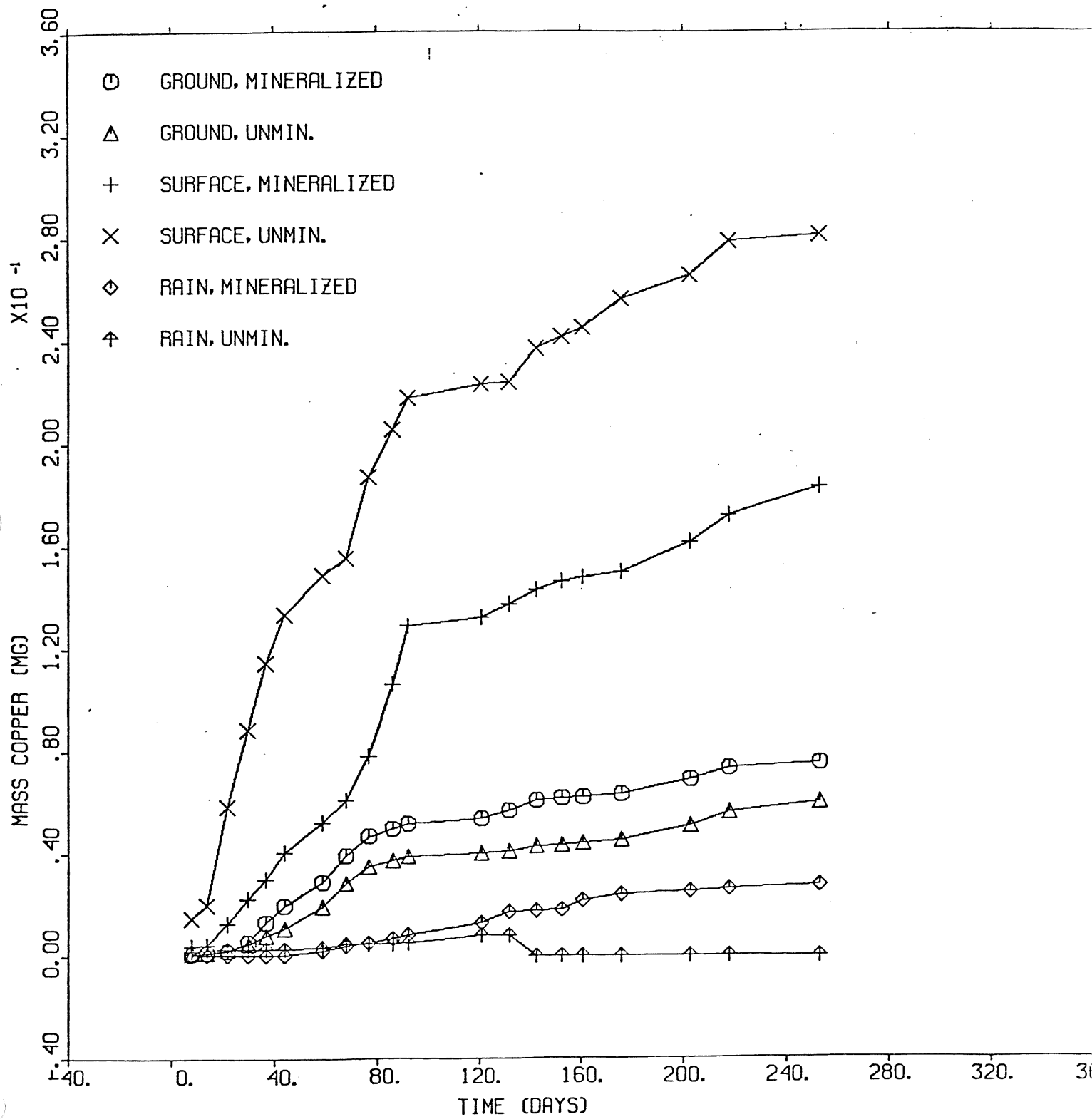
These column leaching studies have proved to be useful complements to batch leaching studies. Behaviors observed in these studies closely approximate results observed in field studies. The most important observations resulting from the column leaching studies are that the parameters monitored in the leachates fell into two distinct categories. The leaching behavior of nickel, cobalt, manganese, and sulfate exhibited a greater dependence on type of gabbro than on type of leaching solution, while copper and iron exhibited just the opposite type of dependence.

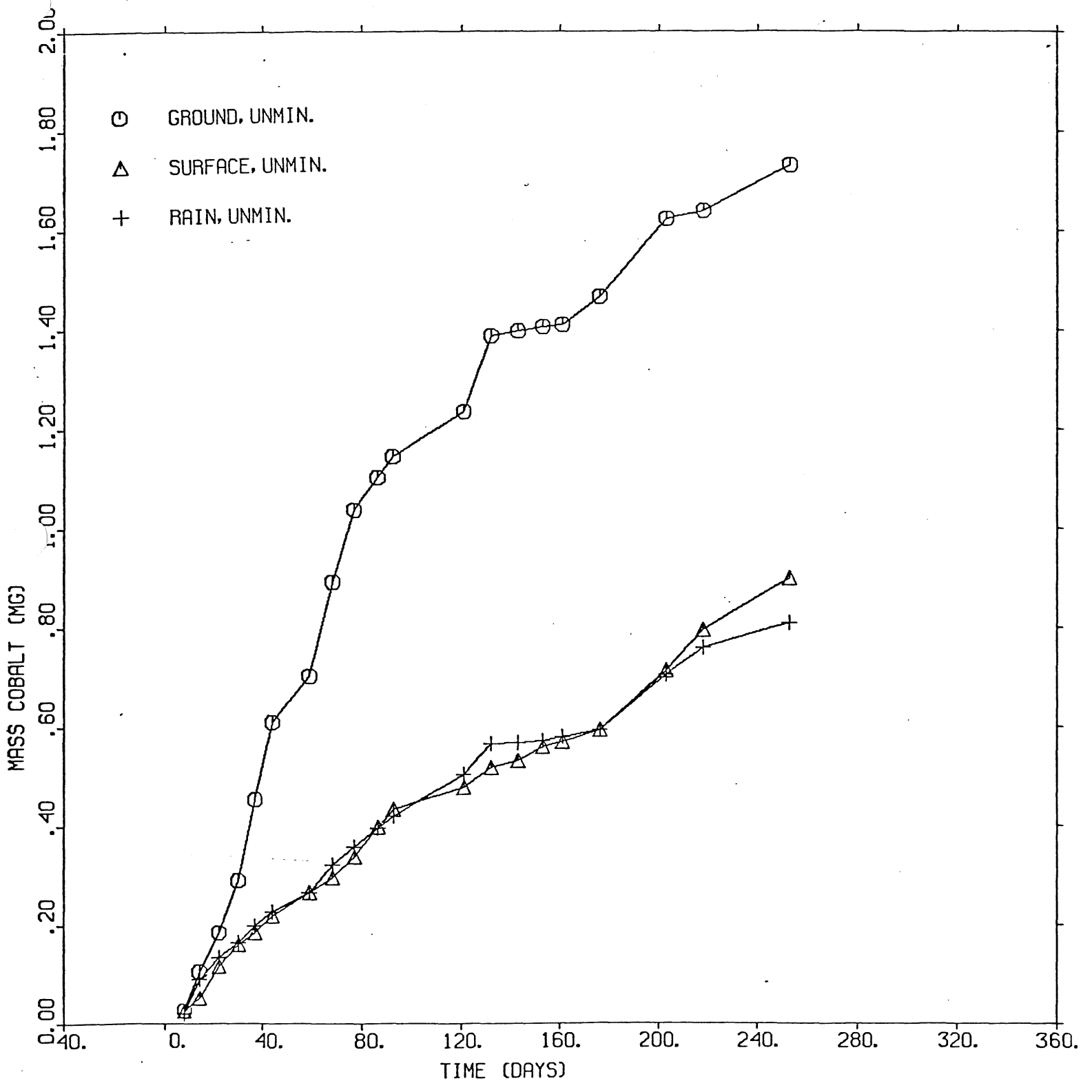
The observation that the surface water was most effective in leaching Cu and Fe may have implications for field studies. The likely reason for this phenomenon is the greater participation of Cu and Fe in complexation reactions with organic ligands such as those present in surface waters, as compared to Ni, Co, and Mn.

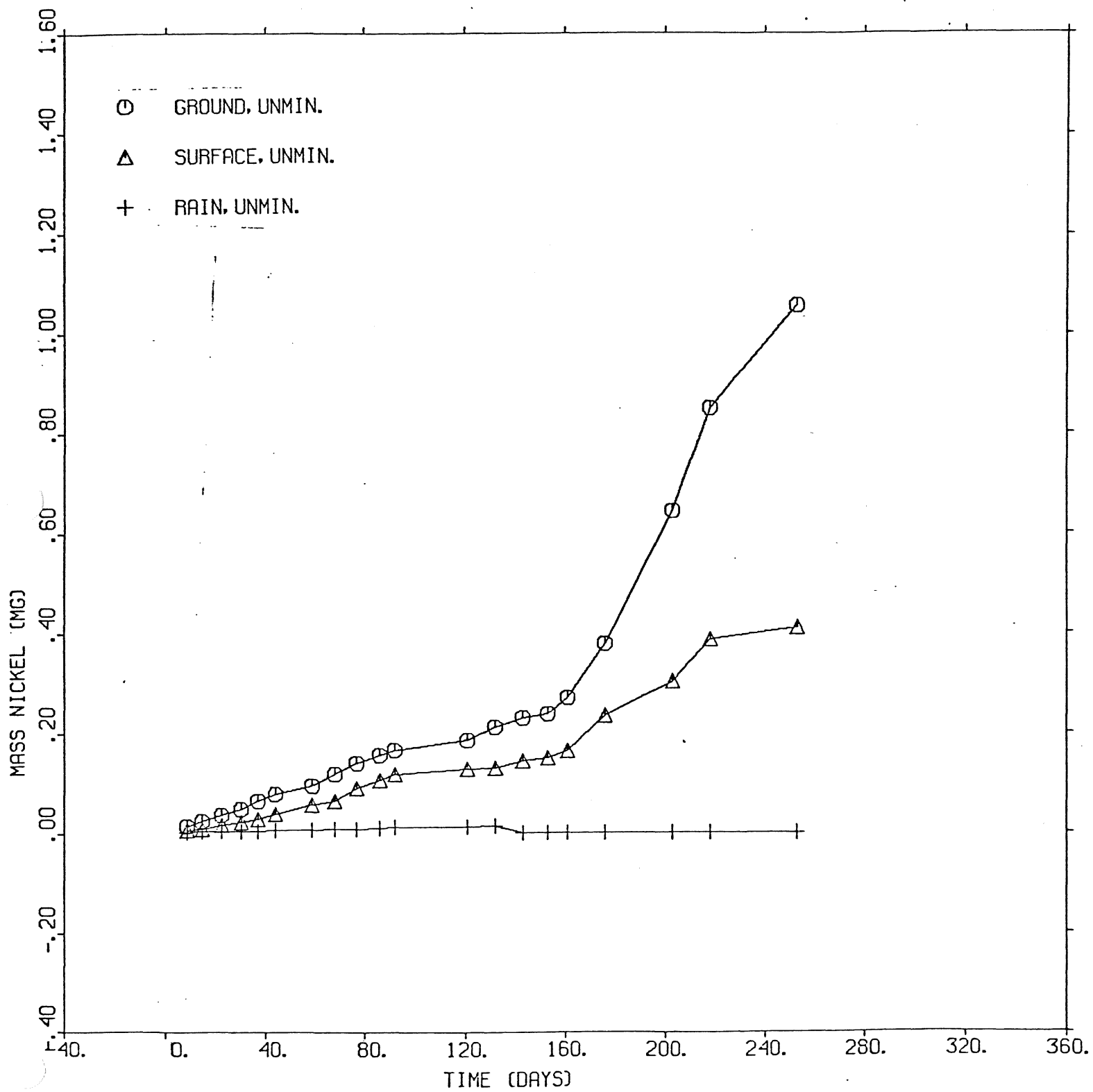
The relatively poor effectiveness of the synthetic rainwater (distilled water) in leaching all the monitored species from gabbro is due to the difference

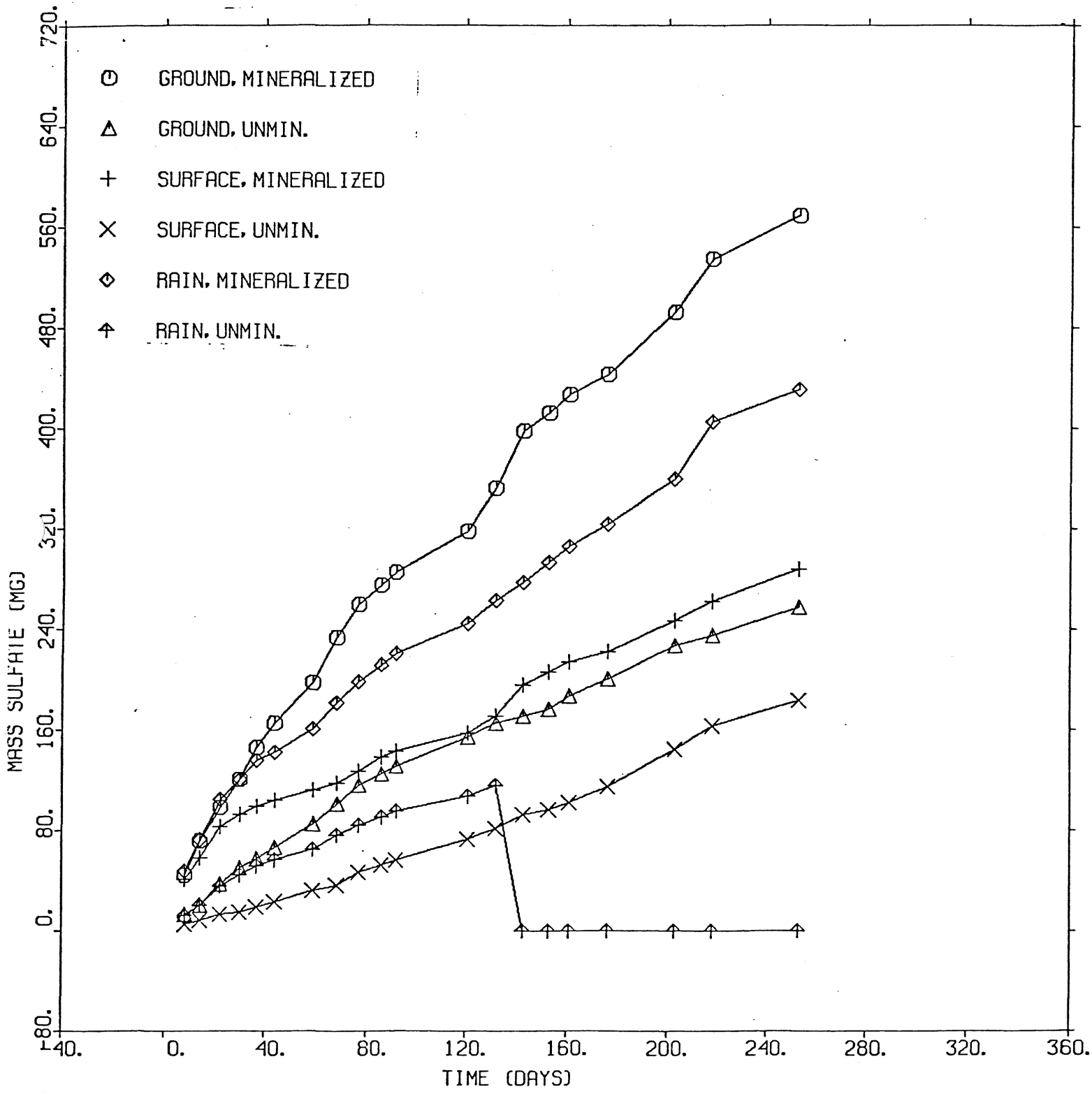
in ionic strengths of the three leaching solutions. None of the original leaching solutions contained heavy metal concentrations approaching solution; therefore, the effect of the higher ionic strengths of the groundwater and surface water was to reduce the magnitude of the ionic activity coefficient for each species, promoting both faster leaching rates and higher equilibrium concentrations of the leached species.

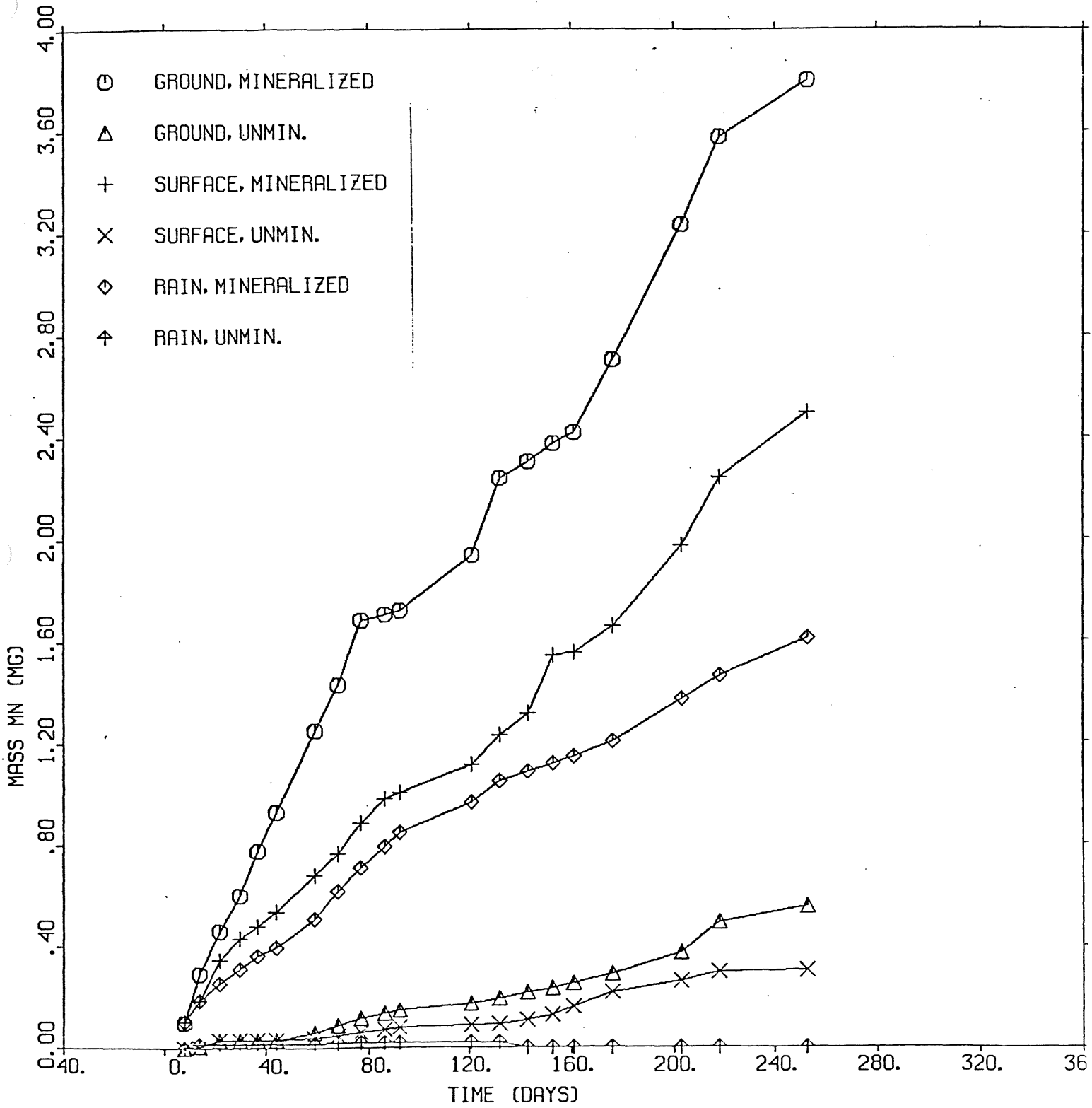


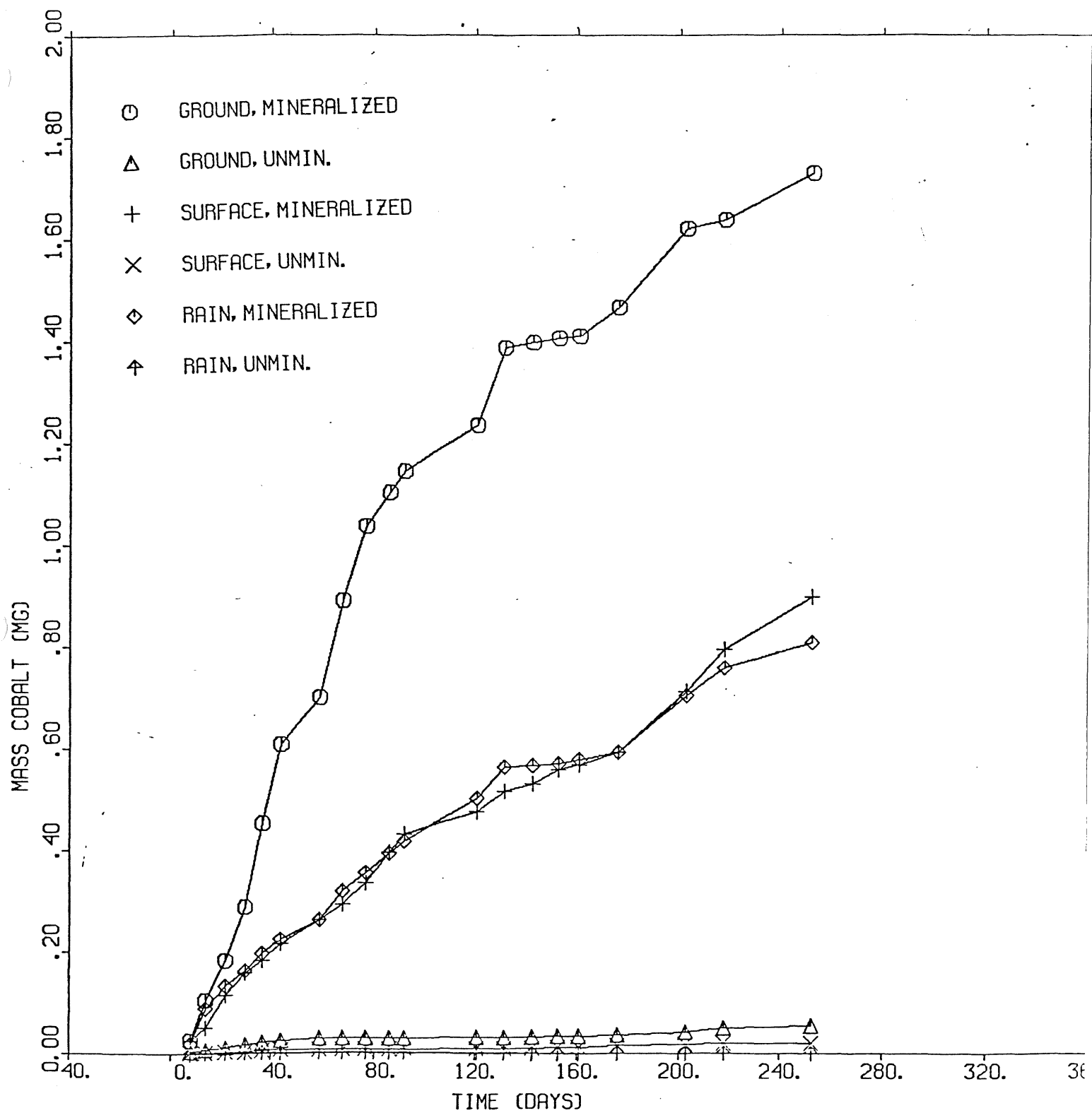


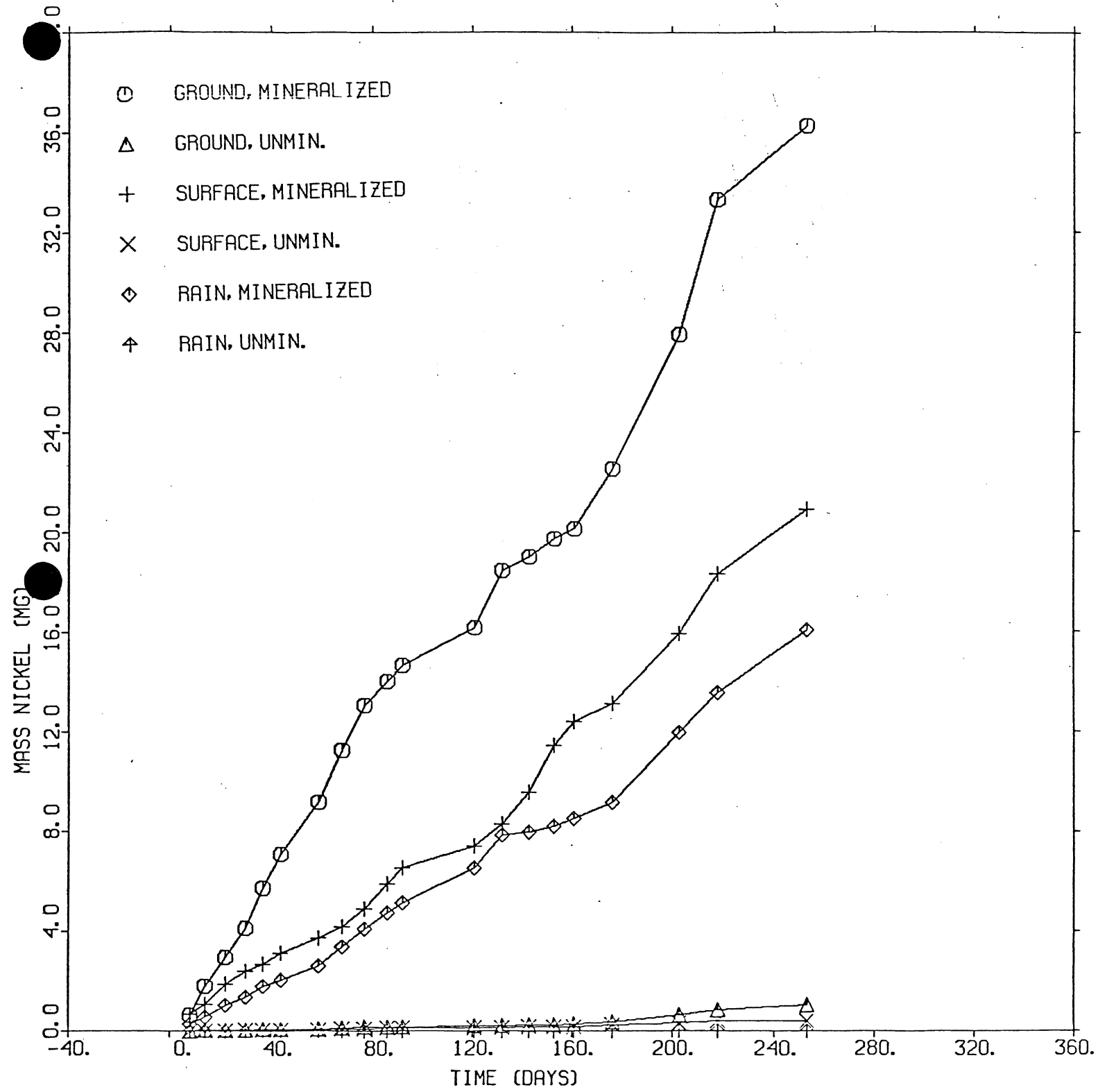












CN 024

ESTIMATES OF SULFATE DEPOSITION
USING A STOCHASTIC MODEL FOR PRECIPITATION

INTRODUCTION

The deposition of acidic sulfates has been shown to be one of the more damaging environmental effects caused by the emission of sulfur dioxide. Estimates of projected sulfate deposition are, therefore, important tools for the impact evaluation of new SO₂ sources (e.g., a copper-nickel smelter).

The purpose of this paper is to derive mathematical formulas for calculating sulfate deposition. Usually these estimates are made using computer simulations. In these simulations the chemical and physical elements of the deposition process are modeled by simple mathematical expressions, where the computer is needed to simulate the varying wind and rain conditions. I propose eliminating the computer by using a simple statistical model for the meteorological variables.

The resulting deposition formulas derived from this statistical model should be adequate for estimating sulfate effects of copper-nickel smelting until more sophisticated computer simulations programs are ready. Beyond that, a closed-form deposition formula can still be useful because of its flexibility. For example, a sensitivity analysis for our deposition estimates can be done almost entirely by mathematical manipulations of the formula, reducing the need for extensive computer runs with different values of the physical parameters.

THEORYBasic Definitions

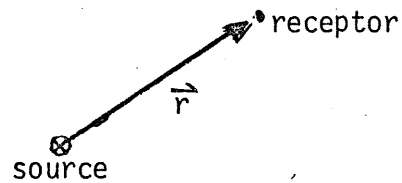
The situation I want to model is a single point source of SO_2 and/or sulfates. (Multiple sources can be modeled by adding the deposition from each individual source.) The desired result will be the total deposition measured as mass of sulfate per unit area. For the statistical approach to work, the length of time over which the sulfate deposition is calculated must be substantial longer than a single storm or other synoptic weather systems event. Yearly loading and seasonal loadings would be the quantities typically derived by this method.

To be precise, define:

$$M_2(\vec{r}, t) \equiv \text{SO}_2 \text{ deposition rate}$$

(units: $\frac{\text{mass SO}_2}{\text{area} \times \text{time}}$)

$$M_4(\vec{r}, t) \equiv \text{SO}_4 \text{ deposition rate}$$

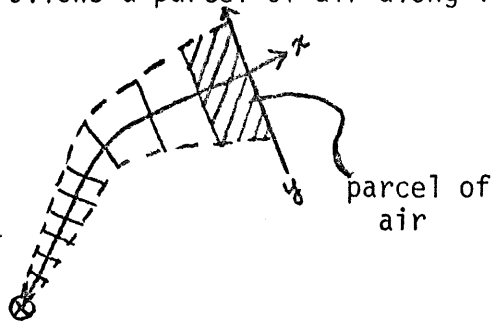


The coordinates (\vec{r}, t) which locate the deposition measurement are an Eulerian coordinate system fixed with respect to the earth. The total deposition in the Eulerian system is now defined by:

$$m_i(\vec{r}) \equiv \int_0^T M_i(\vec{r}, t) dt \quad \text{where } i = 2 \text{ or } 4$$

m_2 and m_4 are the final quantities to be derived.

The derivation starts, however, in a Lagrangian coordinate system, which follows a parcel of air along its trajectory downwind from the source.



The Lagrangian coordinates obviously may vary not only with Lagrangian time τ but also with parcels emitted at different Eulerian times t .

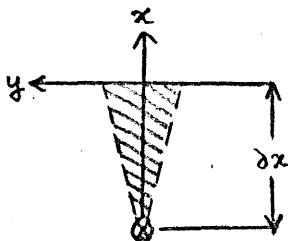
$$\begin{aligned} \tau &\equiv \text{Lagrangian time} \\ &= 0 \text{ at the time of emission} \end{aligned}$$

In the Lagrangian system, the amount of pollutant is measured for a single parcel of air:

$$\begin{aligned} X_i(\tau) &\equiv \text{mass of } SO_i \text{ (} i=2 \text{ or } 4 \text{) in the parcel at time } \tau \\ &\text{(units: } \frac{\text{mass}}{\text{length of parcel}} \text{)} \end{aligned}$$

$$\begin{aligned} D_i(\tau) &\equiv \text{total mass of } SO_i \text{ deposited from the parcel up to time } \tau \\ &\text{(units: mass per length of parcel).} \end{aligned}$$

(The length of the parcel, for purposes of visualization, is defined by the wind speed $u(\tau)$:



$$\delta x = u(\tau) \delta \tau$$

In the end, δx will usually be sent to zero in a limiting procedure.)

At the moment of emission, $X_i(\tau)$ is related to the usual emission rates Q_i (units: mass per unit time):

$$X_i(\tau=0) = u(0) Q_i$$

At any time, X_i and D_i are related by conservation of mass:

$$\begin{aligned} X_2(0) + X_4(0) &= u(0)(Q_2 + Q_4) \\ &= X_2(\tau) + D_2(\tau) + X_4(\tau) + D_4(\tau). \end{aligned}$$

Sulfur Transformation and Removal

(This section is taken from Wendell, Powell, and Drake, 1976)

The sulfate deposition process has three components: dry deposition, rainfall scavenging, and the chemical transformation from SO_2 to SO_4 .

All three components are modeled as first-order processes whose rates are determined by the parameters:

- V_2 = dry deposition velocity for SO_2 (distance/time)
- λ_2 = rainfall scavenging coefficient for SO_2 (time⁻¹)
- V_4 = dry deposition velocity for SO_4 (distance/time)
- λ_4 = rainfall scavenging coefficient for SO_4 (time⁻¹)
- K = first-order rate constant for the oxidation of SO_2 (time⁻¹)
- Δz = plume height or mixing height, whichever is less

Combining all these processes together gives the coupled differential equations:

$$\frac{dX_2}{d\tau} = - \left(\frac{V_2}{\Delta z} + \{\lambda_2\} + k \right) X_2$$

$$\frac{dX_4}{d\tau} = - \left(\frac{V_4}{\Delta z} + \{ \lambda_4 \} \right) X_4 + \frac{M_{SO_4}}{M_{SO_2}} k X_2$$

$$\frac{dD_2}{d\tau} = \left(\frac{V_2}{\Delta z} + \{ \lambda_2 \} \right) X_2$$

$$\frac{dD_4}{d\tau} = \left(\frac{V_4}{\Delta z} + \{ \lambda_4 \} \right) X_4$$

In these equations I have used the notation:

$$\{ \lambda_i \} = \begin{cases} \lambda_i, & \text{if it is raining} \\ 0, & \text{if it is dry} \end{cases}$$

Also, M_{SO_2} and M_{SO_4} are the molecular weights which work out to:

$$\frac{M_{SO_4}}{M_{SO_2}} = \frac{96}{64} = \frac{3}{2}$$

For an arbitrary period of time $[\tau_0, \tau]$, the differential equations for the parcel masses have solutions:

$$X_2(\tau) = X_2(\tau_0) A$$

$$X_4(\tau) = X_4(\tau_0) B + T_{2 \rightarrow 4} X_2(\tau_0) B-A$$

$$\text{where } A \equiv \exp \left[- \left(\frac{V_2}{\Delta z} + \{ \lambda_2 \} + k \right) (\tau - \tau_0) \right]$$

$$B \equiv \exp \left[- \left(\frac{V_4}{\Delta z} + \{ \lambda_4 \} \right) (\tau - \tau_0) \right]$$

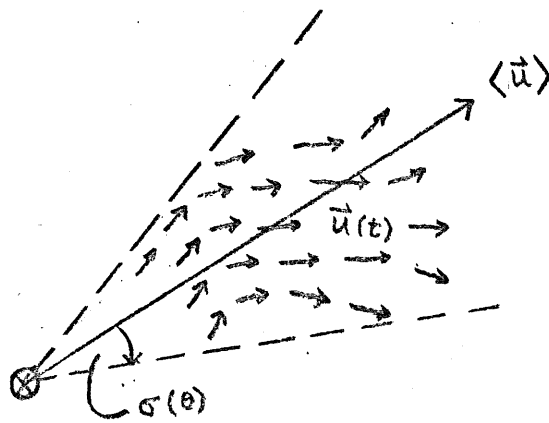
$$T_{2 \rightarrow 4} \equiv \frac{3}{2} k / \left(\frac{V_2 - V_4}{\Delta z} + \{ \lambda_2 - \lambda_4 \} + k \right)$$

Explicit expressions for $D_i(\tau)$ will not be needed.

Converting From Lagrangian to Eulerian Deposition

At a given Lagrangian time τ , the parcel can easily be located in the Eulerian coordinate system. Hence, the Lagrangian deposition rate $dD_i(\tau)/d\tau$ can be roughly equated to the Eulerian counterpart $M_i(\vec{r}, t)$. However, this transformation requires that we first clear up some questions of plume geometry. For me, the simplest geometry comes out of a box model for the dispersion.

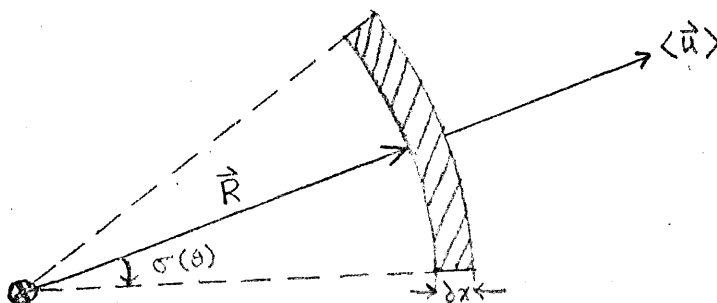
The box is defined for a period of time which would encompass a single synoptic weather system (e.g. the average time between rainfall = 3.4 days).



Average the wind vector field over the entire area of interest covered by the plume over this averaging time. Then, the box is centered about the average wind vector $\langle \vec{u} \rangle$ with a width defined by the standard deviation

of the wind vector headings $\sigma(\theta)$. (An alternative definition of the box width is the average of the $\vec{u}(t)$ components perpendicular to the average $\langle \vec{u} \rangle$.)

Now, the Lagrangian parcel of mass $X_i(\tau)$ is simply the crescent traveling out of the box at a rate $\langle \vec{u} \rangle$. The center of the parcel in Eulerian coordinates is: $\vec{R} = \tau \langle \vec{u} \rangle$.



In the Eulerian system, I can now define a cross-section deposition rate:

$$\bar{M}_i(\vec{R}, t) = |\vec{R}| \int_0^{2\pi} d\theta M_i(\vec{\pi}, t)$$

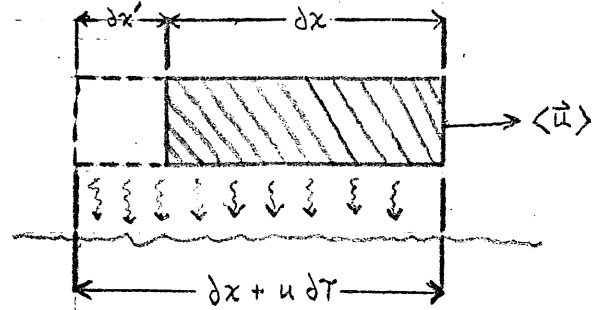
($\frac{\text{mass}}{\text{time} \times \text{distance downwind}}$)

which can be related to the Lagrangian deposition rate.

Recall that the Lagrangian quantity $D_i(\tau) = \frac{\partial m_i}{\partial x}$ in terms of the mass m_i actually deposited. Thus, the deposition rate is:

$$\frac{\partial D_i(\tau)}{\partial \tau} = \frac{\partial^2 m_i}{\partial x \partial \tau}$$

In the Eulerian frame of reference, this mass $\partial^2 m_i$ comes down over a distance equal to the length of the parcel ∂x plus the distance it travels $\partial x' = u \partial \tau$.



Using the fact that time elements are the same in both systems

$$(\partial t = \partial \tau), \bar{M}_i(\vec{R}, t) = \frac{\partial^2 m_i}{(\partial x + u \partial t) \partial t}$$

Picking the differential ∂t so that $u \partial t \ll \partial x$, we get:

$$\begin{aligned} \bar{M}_i(\vec{R}, t) &= \frac{\partial^2 m_i}{\partial x \partial \tau} = \frac{\partial D_i(\tau)}{\partial \tau} \\ &= (v_i / \Delta z + \{\lambda_i\}) X_i(\tau) \end{aligned}$$

where $t = t_{\text{emission}} + \tau$
and $\vec{R} = \tau \langle \vec{u} \rangle$

This relationship relates deposition in the two coordinate systems at any instant.

Statistical Model for the Meteorology

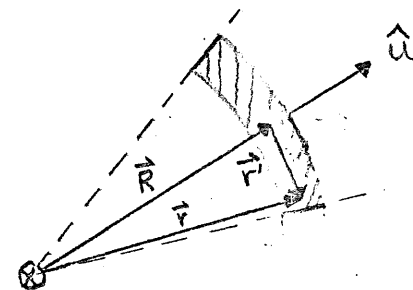
Now we turn to the total deposition over time:

$$M_i(\vec{r}) = \int_0^T M_i(\vec{r}, t) dt$$

To express this in terms of $\bar{M}_i(\vec{R}, t)$, we relate the Lagrangian and Eulerian coordinates by:

$$\begin{aligned} \vec{r} &= \vec{R} + \vec{r}' \\ &= \tau \langle \vec{u} \rangle + \vec{r}' \end{aligned}$$

$$\begin{aligned} \text{Also, } \tau &= |\vec{R}| / |\langle \vec{u} \rangle| \equiv \frac{R}{u} \\ &= r/u \text{ because } |\vec{R}| = |\vec{r}|. \end{aligned}$$



Then, express the horizontal spread of the plume by a function $\phi(\vec{r}')$ (units: distance⁻¹) so that:

$$M_i(\vec{r}, t) = \phi(\vec{r}') \bar{M}_i(\vec{R}, t)$$

(The function $\phi(\vec{r}')$ could be a Gaussian function--the Gaussian plume model--or a constant--the box model.) Thus, I can write:

$$M_i(\vec{r}) = \int_0^T dt \left(\frac{v_i}{\Delta z} + \{\lambda_i\} \right) \phi(\vec{r}') X_i(\tau = r/u)$$

Reviewing this expression for the total deposition, we can see that it contains many meteorological parameters which are implicitly functions of weather changes over time t :

$\langle \vec{u}(t) \rangle$ -- average wind speed and direction

$\{\lambda_i(t)\}$ -- rainfall scavenging coefficient

$\Delta z(t)$ -- mixing height

$\phi(\vec{r}' = \vec{r} - r\hat{u})$ -- plume spread, a function of wind direction:

$$\hat{u}(t) \equiv \langle \vec{u}(t) \rangle / u(t)$$

Instead of a simulation of these meteorological parameters, we replace them with a random variable (terminology?) and the appropriate distribution function.

Mathematically, I'll do this with a Dirac delta function $\delta(x)$ with the property:

$$f[x(t)] = \int dx f(x) \delta(x(t)-x)$$

Therefore,

$$\begin{aligned} m_i(\vec{r}) &= \int_0^T dt \left(\frac{v_i}{\Delta z(t)} + \{ \lambda_i(t) \} \right) \phi(\vec{r} - r \hat{u}(t)) X_i \left[\frac{r}{u(t)}; \{ \lambda_i(t) \}, \Delta z(t) \right] \\ &= \int_0^T dt \int_0^\infty d(\Delta z) \delta(\Delta z(t) - \Delta z) \int_0^\infty d\lambda_2 \delta(\{ \lambda_2(t) \} - \lambda_2) \times \\ &\quad \int_0^\infty d\lambda_4 \delta(\{ \lambda_4(t) \} - \lambda_4) \int_0^\infty du \delta(u(t) - u) \int_0^{2\pi} d\hat{u} \delta(\hat{u}(t) - \hat{u}) \times \\ &\quad \left(\frac{v_i}{\Delta z} + \lambda_i \right) \phi(\vec{r} - r \hat{u}) X_i \left(\frac{r}{u}, \lambda_2, \lambda_4, \Delta z \right) \\ &= \int_0^\infty d(\Delta z) \int_0^\infty d\lambda_2 \int_0^\infty d\lambda_4 \int_0^\infty du \int_0^{2\pi} d\hat{u} \left(\frac{v_i}{\Delta z} + \lambda_i \right) \times \\ &\quad \phi(\vec{r} - r \hat{u}) X_i \left(\frac{r}{u}, \lambda_2, \lambda_4, \Delta z \right) \times \\ &\quad \int_0^T dt \delta(\Delta z(t) - \Delta z) \delta(\{ \lambda_2(t) \} - \lambda_2) \delta(\{ \lambda_4(t) \} - \lambda_4) \times \\ &\quad \delta(u(t) - u) \delta(\hat{u}(t) - \hat{u}). \end{aligned}$$

This last integral defines a statistical distribution function:

$$f(\Delta z, \lambda, \vec{u}) = \frac{1}{T} \int_0^T dt \delta(\Delta z(t) - \Delta z) \delta(\{\lambda_2(t)\} - \lambda_2) \times \\ \delta(\{\lambda_4(t)\} - \lambda_4) \delta(u(t) - u) \delta(\hat{u}(t) - \hat{u})$$

So,

$$m_i(\vec{r}) = T \int d(\Delta z) \int d\lambda_2 \int d\lambda_4 \int du \int d\hat{u} \left(\frac{v_i}{\Delta z} + \lambda_i \right) \phi(\vec{r}) \chi_i\left(\frac{r}{u}\right) f(\Delta z, \lambda, \vec{u})$$

To proceed with this formula, some specific assumptions have to be made about the meteorological statistics.

*Mixing height--Assume that Δz is independent of the other parameters,

i.e.

$$f(\Delta z, \lambda_2, \lambda_4, u, \hat{u}) = g(\Delta z) h(\lambda_2, \lambda_4, u, \hat{u})$$

As for the distribution $g(\Delta z)$, we have data for two approaches:

1st Approximation--use the annual average for Δz and ignore the distribution.

Improvements--divide the year into four seasons and use the seasonal average for each. See Holzworth (1972) for data.

*Wind speed--We do have extensive wind data showing that speed is correlated with wind direction and has a log-normal distribution (geometric mean and standard deviation not yet calculated).

1st Approximation--assume that wind speed is independent of direction, and use the geometric mean for u without any distribution.

Improvements--put in a log-normal distribution and perform the integration over u .

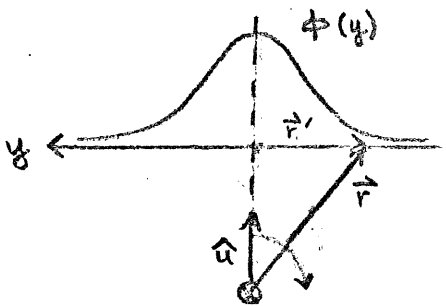
*Wind direction--the wind rose:

$$g(\hat{u}) = \frac{1}{T} \int_0^T dt \delta(\hat{u}(t) - \hat{u})$$

is a crucial statistical distribution, both for the plume spread $\phi(\vec{r}-r\hat{u})$ and for the rainfall scavenging coefficients which have an important correlation with wind direction.

1st Approximation--assume that the rainfall is independent of the wind direction. Then, the integration over \hat{u} only has to include:

$$\int_0^{2\pi} d\hat{u} \phi(\vec{r}-r\hat{u}) g(\hat{u})$$



Assume that the plume is spread over a width that is small both with respect to the radius r (so that the integration over the angle $d\hat{u}$ can be replaced by the linear coordinate $dy = r d\hat{u}$), and also

with respect with the scale of variations in the wind rose (so that the variable quantity $g(\hat{u}) \cong g(\hat{r})$, a constant).

$$\text{Thus, } \int_0^{2\pi} du \phi(\vec{r}-r\hat{u}) g(\hat{u}) \cong g(\hat{r}) \int_{-\infty}^{\infty} \frac{dy}{r} \phi(y)$$

According to the definition of $\phi(y)$, it must be normalized so that:

$$\begin{aligned} \int_{-\infty}^{\infty} dy M_i(\vec{r}, t) &= \int_{-\infty}^{\infty} dy \phi(y) \bar{M}_i(\vec{R}, t) \\ &= \bar{M}_i(\vec{R}, t) \int_{-\infty}^{\infty} dy \phi(y) \\ &= \bar{M}_i(\vec{R}, t) \end{aligned}$$

So,

$$\int_0^{2\pi} d\hat{u} \phi(\vec{r}-r\hat{u}) g(\hat{u}) \cong \frac{g(\hat{r})}{r}$$

Improvements--the major matter of concern is to consider correlation between wind and rain by using a wind-rain rose $g(\hat{u}, \lambda_2, \lambda_4)$. The full implications of this procedure will be discussed below, but as far as plume spread is concerned, the above approximations still all apply so that:

$$\int_0^{2\pi} d\hat{u} \phi(\vec{r} - r\hat{u}) g(\hat{u}, \lambda_2, \lambda_4) \cong \frac{g(\hat{F}, \lambda_2, \lambda_4)}{r}$$

just as before.

*Rainfall--according to my survey of the rainfall scavenging literature, λ_i is a function of the rainfall rate $I \equiv$ mm of rainfall per hour. Of course, λ_i is zero when it is not raining. Thus, two statistical models are needed to handle rainfall:

- 1) Distance the plume travels before it hits rain.
- 2) The rainfall intensity rate during a storm.

On the first question, stochastic theory suggests that the Lagrangian time of travel θ for the parcel before it hits a storm might be given by an exponential distribution:

$$h(\theta) = \omega e^{-\omega\theta}$$

Preliminary precipitation data supports this hypothesis and gives a value for the parameter ω :

$$\omega = \frac{1}{3.43 \text{ days}}$$

where 3.43 days is the arithmetic mean of the time between rain storms. Note that the precipitation data is taken from measuring stations fixed in the Eulerian coordinate system, so in principal, the distribution for the Lagrangian time of travel could be different.

1st Approximation--we assume that the parcel travels until it encounters a storm at time $\tau = \theta$. The storm persists until all the sulfur is washed out of the parcel. (This last assumption is made more palatable by the experimental observation that the sulfate content of rainfall is limited to the first few minutes of rainfall. Thus, the scavenging coefficient is large enough to make the assumption of infinite rainstorms a reasonable one.) Thus, the rainfall scavenging coefficients will have values:

$$\{\lambda_i\} = \left\{ \begin{array}{l} 0, \quad \tau < \theta \\ \lambda_i, \quad \tau \geq \theta \end{array} \right\}$$

In this first approximation, λ_i will be calculated using the arithmetic mean for the rainfall rate. For sulfate, I'm using the formula:

$$\lambda_4 = \frac{3}{4} \frac{I^{3/4}}{0.35} \quad (\text{units: hours}^{-1}) \quad \text{Source: Garland (1977)}$$

Improvements--as usual, the loading estimate can be improved by inserting a distribution function. Rain storms can also be given a finite extent, again using an exponential distribution for their extent in Lagrangian time.

However, the most important improvement is using the wind-rain rose discussed above. The distribution function $g(\hat{r}, \lambda_2, \lambda_4)$ measures the differing probability of hitting rain with different wind directions, and this can be quantified by making the average time of travel ω a function of wind direction r . Thus, I would use the distribution function:

$$\begin{aligned} g(\hat{r}, \lambda_2, \lambda_4) &= g(\hat{r}) h(\theta, \hat{r}) \\ &= g(\hat{r}) \omega(\hat{r}) e^{-\theta \omega(\hat{r})} \end{aligned}$$

Pulling this all together, the first approximation to sulfate loading will be given by:

$$m_i(r) = \tau \int_0^\infty d(\Delta z) \int_0^\infty d\theta \int_0^\infty dI \int_0^\infty du \int_0^{2\pi} d\hat{u} \left(\frac{V_i}{\Delta z} + \{\lambda_i\} \right) \times \\ \phi(\vec{r}') X_i\left(\frac{r}{u}\right) f(\Delta z, \theta, I, u, \hat{u})$$

where $f(z, \theta, I, u, \hat{u}) =$

$$\delta(\Delta z - \bar{\Delta z}) h(\theta) \delta(I - \bar{I}) \delta(u - \bar{u}) g(\hat{u})$$

Taking into account the integration over \hat{u} described earlier, this gives:

$$m_i(\vec{r}) = \frac{\tau g(\hat{r})}{r} \int_0^\infty d\theta h(\theta) \left(\frac{V_i}{\Delta z} + \{\bar{\lambda}_i\} \right) X_i\left(r; \bar{u}, \bar{\Delta z}, \{\bar{\lambda}_i\}\right)$$

Derivation of the Sulfate Deposition Formula

Using the formulas for X_i given in section B, we got:

$$X_2\left(\frac{r}{u}\right) = X_2(0) \exp\left[-\left(\frac{V_2}{\Delta z} + k\right)r/\bar{u}\right] \quad \text{for } \tau = \frac{r}{u} < \theta$$

Define $k_2 = V_2/\Delta z + k$, and use the earlier observation that $X_2(0) = Q_2/\bar{u}$,

so: $X_2\left(\frac{r}{u}\right) = \frac{Q_2}{\bar{u}} \exp(-k_2 r/\bar{u})$ for $\theta > r/\bar{u}$.

Likewise, for $\tau = \frac{r}{u} \gg \theta$,

$$\begin{aligned} X_2\left(\frac{r}{u}\right) &= X_2(\theta) \exp\left[-(k_2 + \bar{\lambda}_2)\left(\frac{r}{u} - \theta\right)\right] \\ &= \frac{Q_2}{\bar{u}} \exp\left[-k_2 \theta\right] \exp\left[-(k_2 + \bar{\lambda}_2)\left(\frac{r}{u} - \theta\right)\right] \\ &= \frac{Q_2}{\bar{u}} \exp\left[-(k_2 + \bar{\lambda}_2)r/\bar{u}\right] \exp\left[\bar{\lambda}_2 \theta\right] \end{aligned}$$

For sulfate,

$$x\left(\frac{r}{\bar{u}}\right) = \frac{Q_4}{\bar{u}} \exp[-k_4 r/\bar{u}] + T_{\text{dry}} \frac{Q_2}{\bar{u}} \left(\exp[-k_4 r/\bar{u}] - \exp[-k_2 r/\bar{u}] \right)$$

for $x/\bar{u} < \theta$. For $x/\bar{u} \geq \theta$ (after the rain starts),

$$X_4\left(\frac{r}{\bar{u}}\right) = \frac{Q_4}{\bar{u}} \exp[-(k_4 + \bar{\lambda}_4) r/\bar{u}] \exp[\bar{\lambda}_4 \theta] \\ + \frac{Q_2}{\bar{u}} \left\{ T_{\text{dry}} \left(\exp[-k_4 \theta] - \exp[-k_2 \theta] \right) \exp[-(k_4 + \bar{\lambda}_4) (\frac{r}{\bar{u}} - \theta)] \right. \\ \left. + T_{\text{wet}} \exp[-k_2 \theta] \left(\exp[-(k_4 + \bar{\lambda}_4) (\frac{r}{\bar{u}} - \theta)] - \exp[-(k_2 + \bar{\lambda}_2) (\frac{r}{\bar{u}} - \theta)] \right) \right\}$$

where $k_4 \equiv v_4/\Delta z$

$$T_{\text{dry}} \equiv \frac{\frac{3}{2} k}{\frac{v_2 - v_4}{\Delta z} + k}$$

$$= \frac{\frac{3}{2} k}{k_2 - k_4} \equiv \frac{3}{2} k / \Delta k$$

$$T_{\text{wet}} \equiv \frac{\frac{3}{2} k}{\Delta k + \lambda_2 - \lambda_4} \equiv \frac{\frac{3}{2} k}{\Delta k + \Delta \lambda}$$

Now substitute this expression for X_2 into the formula for the total SO_2

loading:

$$m_2(\vec{r}) = \frac{T_g(\hat{r})}{r} \cdot \left\{ \int_{r/\bar{u}}^{\infty} d\theta \omega e^{-\omega \theta} \frac{v_2}{\Delta z} \times \frac{Q_2}{\bar{u}} \exp[-k_2 r/\bar{u}] \right. \\ \left. + \int_0^{r/\bar{u}} d\theta \omega e^{-\omega \theta} \left(\frac{v_2}{\Delta z} + \bar{\lambda}_2 \right) \frac{Q_2}{\bar{u}} \exp[-(k_2 + \bar{\lambda}_2) r/\bar{u}] \exp[\bar{\lambda}_2 \theta] \right\} \\ = \frac{\omega Q_2 T_g(\hat{r})}{r \bar{u}} \left\{ \frac{v_2}{\Delta z} \exp[-k_2 r/\bar{u}] \int_{r/\bar{u}}^{\infty} d\theta e^{-\omega \theta} \right. \\ \left. + \left(\frac{v_2}{\Delta z} + \bar{\lambda}_2 \right) \exp[-(k_2 + \bar{\lambda}_2) r/\bar{u}] \int_0^{r/\bar{u}} d\theta e^{-(\omega - \bar{\lambda}_2) \theta} \right\}$$

In general, these exponential integrals have the values:

$$\int_{r/\bar{u}}^{\infty} d\theta e^{-A\theta} = \frac{1}{A} e^{-Ar/\bar{u}}$$

$$\int_0^{r/\bar{u}} d\theta e^{-B\theta} = \frac{1}{B} (1 - e^{-Br/\bar{u}})$$

Therefore,

$$M_2(\vec{r}) = \frac{\omega Q_2 T_g(\vec{r})}{r\bar{u}} \left\{ \frac{v_2}{\omega \Delta z} \exp[-(\kappa_2 + \omega)r/\bar{u}] \right. \\ \left. + \frac{v_2/\Delta z + \bar{\lambda}_2}{\omega - \bar{\lambda}_2} \exp[-(\kappa_2 + \bar{\lambda}_2)r/\bar{u}] (1 - \exp[-(\omega - \bar{\lambda}_2)r/\bar{u}]) \right\}$$

$$M_2(\vec{r}) = \frac{\omega Q_2 T_g(\vec{r})}{r\bar{u}} \left\{ \frac{v_2}{\omega \Delta z} e^{-K_{2D} r/\bar{u}} \right. \\ \left. + \frac{v_2/\Delta z + \bar{\lambda}_2}{\omega - \bar{\lambda}_2} (e^{-K_{2W} r/\bar{u}} - e^{-K_{2D} r/\bar{u}}) \right\}$$

where $K_{2D} \equiv \kappa_2 + \omega$ (rate of dry SO_2 deposition)

$K_{2W} \equiv \kappa_2 + \bar{\lambda}_2$ (rate of wet SO_2 deposition)

total deposition of SO_2

Turning to the sulfate deposition:

$$M_4(r) = \frac{\omega T_g(r)}{r\bar{u}} \left\{ \frac{Q_4 V_4}{\omega \Delta z} e^{-K_{4D} r/\bar{u}} + \frac{Q_4 (v_4/\Delta z + \bar{\lambda}_4)}{\omega - \bar{\lambda}_4} (e^{-K_{4W} r/\bar{u}} - e^{-K_{4D} r/\bar{u}}) \right. \\ \left. + Q_2 T_{dry} \frac{v_4}{\Delta z} (\exp[-\kappa_4 r/\bar{u}] - \exp[-\kappa_2 r/\bar{u}]) \int_{r/\bar{u}}^{\infty} d\theta e^{-\omega\theta} \right. \\ \left. + Q_2 \left(\frac{v_4}{\Delta z} + \bar{\lambda}_4 \right) T_{dry} \exp[-(\kappa_4 + \bar{\lambda}_4)r/\bar{u}] \left\{ \int_0^{r/\bar{u}} d\theta \exp[-\omega\theta - \kappa_4\theta + (\kappa_4 + \bar{\lambda}_4)\theta] \right. \right. \\ \left. \left. - \int_0^{r/\bar{u}} d\theta \exp[-\omega\theta - \kappa_2\theta + (\kappa_4 + \bar{\lambda}_4)\theta] \right\} \right. \\ \left. + Q_2 \left(\frac{v_4}{\Delta z} + \bar{\lambda}_4 \right) T_{wet} \left\{ \exp[-(\kappa_4 + \bar{\lambda}_4)r/\bar{u}] \int_0^{r/\bar{u}} \exp[-\omega\theta - \kappa_2\theta + (\kappa_4 + \bar{\lambda}_4)\theta] \right. \right. \\ \left. \left. - \exp[-(\kappa_2 + \bar{\lambda}_2)r/\bar{u}] \int_0^{r/\bar{u}} \exp[-\omega\theta - \kappa_2\theta + (\kappa_2 + \bar{\lambda}_2)\theta] \right\} \right\}$$

where $K_{4D} = V_4/\Delta z + \omega$ and $K_{4W} = V_4/\Delta z + \lambda_4$ are defined by analogy to the SO_2 derivation. Substituting the expression for the integrals:

$$\begin{aligned} \eta_4(\vec{r}) = \frac{wTg(\hat{r})}{r\bar{u}} & \left\{ \text{terms proportional to } Q_4 + \frac{Q_2 T_{dry} V_4}{\omega \Delta z} (e^{-K_{4D} r/\bar{u}} - e^{-K_{2D} r/\bar{u}}) \right. \\ & + Q_2 T_{dry} \left(\frac{V_4}{\Delta z} + \bar{\lambda}_4 \right) \exp[-(K_4 + \bar{\lambda}_4) r/\bar{u}] \left\{ \frac{1}{\omega - \bar{\lambda}_4} (1 - \exp[-(\omega - \bar{\lambda}_4) r/\bar{u}]) \right. \\ & \quad \left. - \frac{1}{\omega + K_2 - K_4 - \bar{\lambda}_4} (1 - \exp[-(\omega + K_2 - K_4 - \bar{\lambda}_4) r/\bar{u}]) \right. \\ & + Q_2 T_{wet} \left(\frac{V_4}{\Delta z} + \bar{\lambda}_4 \right) \left\{ \frac{\exp[-(K_4 + \bar{\lambda}_4) r/\bar{u}]}{\omega + K_2 - K_4 - \bar{\lambda}_4} (1 - \exp[-(\omega + K_2 - K_4 - \bar{\lambda}_4) r/\bar{u}]) \right. \\ & \quad \left. - \frac{\exp[-(K_2 + \bar{\lambda}_2) r/\bar{u}]}{\omega - \bar{\lambda}_2} (1 - \exp[-(\omega - \bar{\lambda}_2) r/\bar{u}]) \right\} \left. \right\} \end{aligned}$$

$$\begin{aligned} \eta_4(\vec{r}) = \frac{\omega Tg(\hat{r})}{r\bar{u}} & \left\{ \text{terms proportional to } Q_4 + \text{dry deposition terms for } Q_2 \right. \\ & + Q_2 \left(\frac{V_4}{\Delta z} + \bar{\lambda}_4 \right) \left\{ \frac{T_{dry}}{\omega - \bar{\lambda}_4} (e^{-K_{4W} r/\bar{u}} - e^{-K_{4D} r/\bar{u}}) \right. \\ & \quad - \frac{T_{dry}}{\omega + K_2 - \bar{\lambda}_4} (e^{-K_{4W} r/\bar{u}} - e^{-K_{2D} r/\bar{u}}) + \frac{T_{wet}}{\omega + K_2 - \bar{\lambda}_4} (e^{-K_{4W} r/\bar{u}} - e^{-K_{2D} r/\bar{u}}) \\ & \quad \left. - \frac{T_{wet}}{\omega - \bar{\lambda}_2} (e^{-K_{2W} r/\bar{u}} - e^{-K_{2D} r/\bar{u}}) \right\} \left. \right\} \end{aligned}$$

One final simplification combines the 2nd and 3rd terms in the wet deposition for Q_2 :

$$\frac{T_{\text{wet}} - T_{\text{dry}}}{\omega + \Delta k - \lambda_4} (e^{-K_{4w}r/\bar{u}} - e^{-K_{2D}r/\bar{u}}) = \frac{\frac{3}{2}k(\Delta k - \Delta k - \Delta\lambda)}{\Delta k(\Delta k + \Delta\lambda)(\omega + \Delta k - \lambda_4)} (e^{-K_{4w}r/\bar{u}} - e^{-K_{2D}r/\bar{u}})$$

Combining all terms gives:

$$\begin{aligned} m_4(r) = & \frac{\omega T g(r)}{r \bar{u}} \left\{ \frac{Q_4 v_4}{\omega \Delta z} e^{-K_{4D}r/\bar{u}} \right. \\ & + \frac{Q_4 (v_4/\Delta z + \lambda_4)}{\omega - \lambda_4} (e^{-K_{4w}r/\bar{u}} - e^{-K_{4D}r/\bar{u}}) \\ & + \frac{\frac{3}{2}k Q_2 v_4}{\omega \Delta k \Delta z} (e^{-K_{4D}r/\bar{u}} - e^{-K_{2D}r/\bar{u}}) \\ & + \frac{\frac{3}{2}k Q_2 (v_4/\Delta z + \lambda_4)}{\Delta k(\omega - \lambda_4)} (e^{-K_{4w}r/\bar{u}} - e^{-K_{4D}r/\bar{u}}) \\ & - \frac{\Delta\lambda}{\Delta k(\Delta k + \Delta\lambda)(\omega + \Delta k - \lambda_4)} (e^{-K_{4w}r/\bar{u}} - e^{-K_{2D}r/\bar{u}}) \\ & \left. - \frac{1}{(\omega - \lambda_2)(\Delta k + \Delta\lambda)} (e^{-K_{2w}r/\bar{u}} - e^{-K_{2D}r/\bar{u}}) \right\} \end{aligned}$$

deposition as sulfate.

Simple Approximation for the Sulfate Deposition

The most likely values for the physical parameters allows us to make considerable simplifications in these formulas. A typical set of values (taken mainly from Garland, 1977) is:

$$\lambda_2 = 3.5 \times 10^{-4} \text{ sec}^{-1}$$

$$\lambda_4 = 5.95 \times 10^{-4} \bar{I}^{3/4} \text{ sec}^{-1}$$

$$= 3.35 \times 10^{-3} \text{ sec}^{-1} \text{ for } \bar{I} = 10 \frac{\text{mm}}{\text{hr.}} \text{ as measured at the Kawishiwi Lab}$$

$$V_2 = 0.8 \text{ cm./sec.}$$

$$V_4 \approx \text{an order of magnitude less than } V_2$$

$$\Delta z = 1200 \text{ meters}$$

$$\omega = 1/3.43 \text{ days} = 3.37 \times 10^{-6} \text{ sec}^{-1}$$

$$k = 2\% \text{ hr}^{-1} = 5.56 \times 10^{-6} \text{ sec}^{-1}$$

$$u = 3.95 \text{ m./sec. as measured at Hibbing}$$

With these parameter values,

$$K_{4W} = \frac{V_4}{\Delta z} + \lambda_4 = \mathcal{O}(10^{-7}) + \mathcal{O}(10^{-3}) \approx \lambda_4$$

$$K_{4D} = \frac{V_4}{\Delta z} + \omega = \mathcal{O}(10^{-7}) + \mathcal{O}(10^{-6}) \approx \omega$$

$$K_{2W} = \frac{V_2}{\Delta z} + k + \lambda_2 = \mathcal{O}(10^{-6}) + \mathcal{O}(10^{-6}) + \mathcal{O}(10^{-4}) \approx \lambda_2$$

$$K_{2D} = \frac{V_2}{\Delta z} + k + \omega = \mathcal{O}(10^{-6}) + \mathcal{O}(10^{-6}) + \mathcal{O}(10^{-6})$$

and has no simplification.

These exponents are all an order of magnitude apart, and even the smallest ($K_{4D} \approx \mathcal{O}(10^{-6})$) will lead to $Kr/u > 1$ for r at the large end of our deposition modeling ($r > 1000 \text{ Km.}$). Thus, the differences between exponentials can always be approximated by a single term for large r ,

e.g.

$$e^{-k_{4D} r/u} - e^{-k_{2D} r/\bar{u}} = e^{-\mathcal{O}(10)} - e^{-\mathcal{O}(100)} \quad \text{for } r = 1000 \text{ Km}$$

$$\approx e^{-\omega r/u}$$

Approximations can also be made for many terms appearing in the coefficients,

e.g. $\Delta\lambda = \lambda_2 - \lambda_4 \approx -\lambda_4$

$$v_2/\Delta z + \lambda_4 \approx \lambda_2$$

$$v_4/\Delta z + \lambda_4 \approx \lambda_4$$

$$\Delta k + \Delta\lambda \approx -\lambda_4$$

$$\omega - \lambda_2 \approx -\lambda_2$$

$$\omega - \lambda_4 \approx -\lambda_4$$

$$\omega + \Delta k - \lambda_4 \approx -\lambda_4$$

For SO_2 deposition, these simplifications give:

$$M_2(\vec{r}) \approx \frac{Q_2 T_g(\hat{r})}{r u} \left\{ \frac{\omega v_2}{\omega \Delta z} e^{-k_{2D} r/u} \right.$$

$$\left. + \frac{\omega \lambda_2}{(-\lambda_2)} \left(e^{-\lambda_4 r/u} - e^{-k_{2D} r/u} \right) \right.$$

↑ negligible

$$M_2(\vec{r}) \approx \frac{Q_2 T_g(\hat{r})}{r u} \left(\frac{v_2}{\Delta z} + \omega \right) e^{-k_{2D} r/u}$$

For sulfate,

$$M_4(\vec{r}) \approx \frac{T_g(\hat{r})}{r u} \left\{ \frac{\omega Q_4 v_4}{\omega \Delta z} e^{-\omega r/u} + \frac{\omega Q_4 \lambda_4}{(-\lambda_4)} \left(-e^{-\omega r/u} \right) \right.$$

$$\left. + \frac{3}{2} k Q_2 \omega \left\{ \frac{v_4}{\omega \Delta k \Delta z} e^{-\omega r/u} + \frac{\lambda_4}{\Delta k (-\lambda_4)} \left(-e^{-\omega r/u} \right) \right. \right.$$

$$\left. - \frac{\lambda_4 (-\lambda_4)}{\Delta k (-\lambda_4) (-\lambda_4)} \left(-e^{-k_{2D} r/u} \right) - \frac{\lambda_4}{(-\lambda_2) (-\lambda_4)} \left(-e^{-k_{2D} r/u} \right) \right\}$$

$$M_4(\vec{r}) \approx \frac{Tg(\hat{r})}{ru} \left\{ Q_4 \left(\frac{v_4}{\Delta z} + \omega \right) e^{-\omega r/u} + \frac{3}{2} \frac{k Q_2}{\Delta k} \left(\frac{v_4}{\Delta z} + \omega \right) e^{-\omega r/u} + \frac{3}{2} k \omega Q_2 \left(\frac{1}{\lambda_2} - \frac{1}{\Delta k} \right) e^{-k_{2D} r} \right\}$$

negligible
negligible

Since $e^{-\omega r/u} \gg e^{-k_{2D} r/u}$ for large r , the last term in the above formula is negligible, which leaves:

$$M_4(\vec{r}) \approx \frac{Tg(\hat{r})\omega}{ru} \left(Q_4 + \frac{3k}{\Delta k} Q_2 \right) e^{-\omega r/u}$$

$$\text{Using } \Delta k = \frac{v_2 - v_4}{\Delta z} + k \approx \frac{v_2}{\Delta z} + k,$$

$$M_4(\vec{r}) \approx \frac{Tg(\hat{r})\omega}{ru} \left(Q_4 + \frac{3}{2} \frac{Q_2}{1 + v_2/k \Delta z} \right) e^{-\omega r/u}$$

In the ground, the biota and the waters, SO_2 is ultimately converted to sulfate (although the proportion lost is a matter of conjecture). Thus, the total sulfate deposition can be defined by:

$$M_T(\vec{r}) \equiv \frac{3}{2} M_2(\vec{r}) + M_4(\vec{r})$$

$$\approx \frac{3}{2} \frac{Q_2 T g(\hat{r})}{ru} \left[\left(\frac{v_2}{\Delta z} + \omega \right) e^{-k_{2D} r/u} + \frac{\omega}{1 + v_2/k \Delta z} e^{-\omega r/u} \right]$$

where $Q_4=0$ for simplicity.

From this formula, the dominance of deposition as sulfate can be seen for large r . The cross-over point where the two deposition mechanisms are equal is given by:

$$\ln \left(\frac{v_2}{\Delta z} + \omega \right) - k_{2D} r_x/u = \ln \left(\frac{\omega}{1 + v_2/k \Delta z} \right) - \omega r_x/u$$

$$\begin{aligned}
 \therefore r_x &= \frac{u}{K_{2D} - \omega} \ln \left[\left(1 + \frac{v_2}{\omega \Delta z} \right) \left(1 + \frac{v_2}{K \Delta z} \right) \right] \\
 &= \frac{u}{K + v_2 / \Delta z} \ln \left[\left(1 + \frac{v_2}{\omega \Delta z} \right) \left(1 + \frac{v_2}{K \Delta z} \right) \right] \\
 &= 582 \text{ Km from the parameters given above.}
 \end{aligned}$$

The formula for $M_T(\vec{r})$ is also useful in estimating the range out to which the loading from a single source might be significant. For one measure, take the distance r_{95} at which 95% of the total mass has been deposited. Roughly speaking, r_{95} can be estimated from the fact that $e^{-3} = (1 - .95)$, so

$$\begin{aligned}
 \omega r_{95} / u &\cong 3 \\
 \text{or } r_{95} &= \frac{3u}{\omega} = 2840 \text{ Km}
 \end{aligned}$$

Because of the $\frac{1}{r}$ factor, the deposition rate will be very small at that distance.

Short-range behavior: for small r , many of the same approximations still apply with the one exception of the exponentials. The lower bound for the models applicability is $r = 10 \text{ Km} = 10^4 \text{ meters}$. At this distance the wet deposition exponents $K_{2W}r/u$ and $K_{4W}r/u$ are still $\mathcal{O}(1-10)$, and thus still negligible in the differences with the dry deposition exponentials. On the other hand, $K_{2D}r/u$ and $K_{4D}r/u \cong w$ are now $\mathcal{O}(0.1-0.01)$, so I can use the approximation:

$$e^{-Kr/u} \cong 1 - Kr/u \quad \text{For } \frac{Kr}{u} \ll 1$$

Thus,

$$\begin{aligned}
 M_2(\vec{r}) &\cong \frac{Q_2 T g(\hat{r})}{ru} \left(\frac{v_2}{\Delta z} + \omega \right) \left(1 - \frac{K_{2D}r}{u} \right) \\
 &\cong \frac{Q_2 T g(\hat{r})}{ru} \left(\frac{v_2}{\Delta z} + \omega \right)
 \end{aligned}$$

↖ negligible

which is a hyperbolic curve around $r=10\text{Km}$.

For the sulfate, I'll again use $Q_4 = 0$ which gives:

$$\begin{aligned}
 M_{(4)}^*(r) &\approx \frac{\frac{3}{2} \Phi_2 T g(\hat{r}) \omega k}{ru} \left\{ \frac{v_4}{\omega \Delta z \Delta k} \left(1 - \frac{\omega r}{u} - 1 + \frac{K_{2D} r}{u} \right) \right. \\
 &\quad + \frac{\lambda_4}{\Delta k (-\lambda_4)} \left(-1 + \frac{\omega r}{u} \right) - \frac{\lambda_4 (-\lambda_4)}{\Delta k (-\lambda_4) (-\lambda_4)} \left(-1 + \frac{K_{2D} r}{u} \right) \\
 &\quad \left. - \frac{\lambda_4}{(-\lambda_2) (-\lambda_4)} \left(-1 + \frac{K_{2D} r}{u} \right) \right\} \\
 &\approx \frac{\frac{3}{2} \Phi_2 T g(\hat{r}) \omega k}{ru} \left\{ \frac{v_4}{\omega \Delta z \Delta k} (K_{2D} - \omega) \frac{r}{u} \right. \\
 &\quad \left. + \frac{1}{\Delta k} \left(1 - \frac{\omega r}{u} - 1 + \frac{K_{2D} r}{u} \right) + \frac{1}{\lambda_2} \left(1 - \frac{K_{2D} r}{u} \right) \right\} \\
 &\approx \frac{\frac{3}{2} \Phi_2 T g(\hat{r}) \omega k}{u^2} \left[\frac{v_4}{\omega \Delta z} + 1 + \frac{1}{\lambda_2} \left(\frac{u}{r} - K_{2D} \right) \right] \\
 &\approx \frac{\frac{3}{2} \Phi_2 T g(\hat{r}) \omega k}{u^2} \left(1 + \frac{u}{\lambda_2 r} \right)
 \end{aligned}$$

$\nearrow \approx \Delta k$
 \nwarrow negligible

which is again a hyperbolic curve with r .

At this limit, the total deposition is:

$$M_T(r) = \frac{3}{2} \Phi_2 T \frac{g(\hat{r})}{u} \left[\frac{1}{r} \left(\frac{v_2}{\Delta z} + \omega \right) + \frac{\omega k}{u} \left(1 + \frac{u}{\lambda_2 r} \right) \right]$$

Thus, deposition as sulfate is less than deposition as SO_2 by $\sigma(k/\lambda_2) = \sigma(10^{-2})$ at the small r limit.